## Chapter II

## Historical

1. The investigation of chemical constituents in Andrographis paniculata Nees.

Chemical constituents isolated from this plant have been reported such as lactone, flavone and miscellaneous compound. The occurrence of chemical constituents in Andrographis paniculata are shown.

Table 1. Chemical constituents in Andrographis paniculata Nees

| Type of compound | Compound | Part of the plant | References |
|---|---|---|---|
| Lactone | Andrographolide | leaves, root, whole plant stem | Cava et al, (1962) |
| | Neoandrographolide | leaves, whole plant | Chan et al, (1971) |
| | Deoxyandrographolide-19 β-D-glucoside | leaves | Weimins and Xiaotian, (1982) |
| | 14-Deoxy-11,12 didehydro andrographolide | Whole plant | Balmain and connolly, (1973), |
| | 14-Deoxyandrographolide | leaves, whole plant | Fujita et al (1984) |

| Type of compound | Compound | Part of the plant | References |
|---|---|---|---|
| | 14-Deoxyandro-graphoside | stem | Balmain and Connolly (1973) |
| | Andrograpanin | leaves | Fujita et al, (1984) |
| Lactone | 14-Deoxy-11-Oxoandrogra-pholide | Whole plant | Balmain and Connolly, (1973) |
| | Paniculide A | leave, tissue culture | Allison et al, (1968) |
| | Paniculide B | leave, tissue culture | Allison et al, (1968) |
| | Paniculide C | leave, tissue culture | Allison et al, (1968) |
| Flavone | Andrographin | root | Biswas, Ali and Choudhury (1972) |
| | Panicolin | root | Biswas, Ali and Choudhury (1972) |
| | Mono-O-Methy-wightin | root | Biswas, Ali and Choudhury (1972) |
| | Apigenin-4′,7′ dimethyl ether | root | Biswas, Ali and Choudhury (1972) |
| | Apigenin-4′,7′-di-o-methyl ether | root | Biswas, Ali and Choudhury (1972) |
| | 5-Hydroxy-2′,3′, 7,8-tetramethoxy flavone | root | Gupta et al, (1983) |

| Type of compound | Compound | Part of the plant | References |
|---|---|---|---|
| | 5-hydroxy-7,8-dimethoxy flavone | root | Gupta et al, (1983) |
| | (di)-5-hydroxy-7,8-dimethoxy flavone | root | Gupta et al, (1983) |
| | Andrographidine B,C,D,E and F | leaves | Kuroyanogi et al,(1987) |
| Miscellaneous | | | |
| | 2-Cis-6-tran Farnesol | Whole plant | Overton and Robert,(1974) |
| | 2-trans-6-trans Farnesol | Whole plant | Overton and Robert,(1974) |
| | Caffic acid (3, 4-dihydro cycinnamic acid) | leaves | Satyanarayana, Mythirayee and Krishnamurthy, (1978) |
| | Chlorogenic acid | leaves | Satyanarayana, Mythirayee and Krishnamurthy, (1978) |
| | 3,5-Dicaffeoyl-d quinic acid | leaves | Satyanarayana, Mythirayee and Krishnamurthy, (1978) |
| | $KH_2PO_4$ | whole plant | Gupta et al, (1983) |

The main constituents in aerial part of Andrographis paniculata Nees are diterpenoid lactone compounds that have not been found in other Andrographis species and have been of interest in their pharmacological action.

## 2. Diterpenoid lactone compounds

The term diterpenoid is used here to refer of substances for which at least a portion of the substance clearly originates as a diterpene, but where other biogenetic modifications have altered the structure so that it contains fewer or more than 20 carbon atoms.

Diterpenoid lactone compounds have been isolated from terrestrial higher and lower plant and also marine natural source. There is no completely satisfactory classification of the diterpenoid lactones. The structure of these compounds found in natural source are generally classified as follow.

1. Phytane type diterpenoid lactone

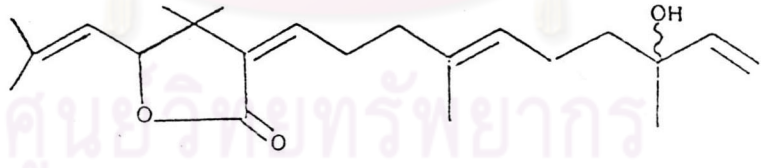


Naviculide (Toyota, Nagashima and Asakawa, 1989) (Porella navicularis)

2. Labdane type diterpenoid lactone

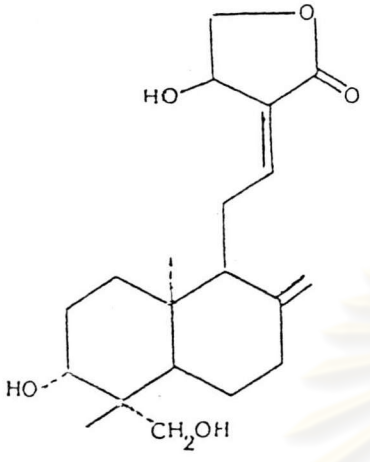

Andrographolide
(Cava et al, 1962)
(Andrographis paniculata)

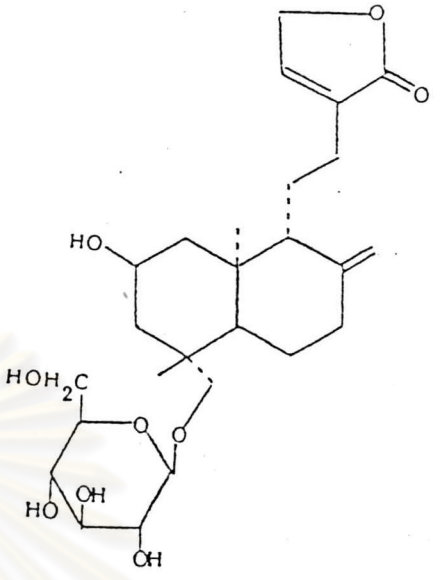

Phloganthoside
(Barua, 1987)
(Phlogacanthus thyrsiflorus)

3. Clerodane type diterpenoid lactone

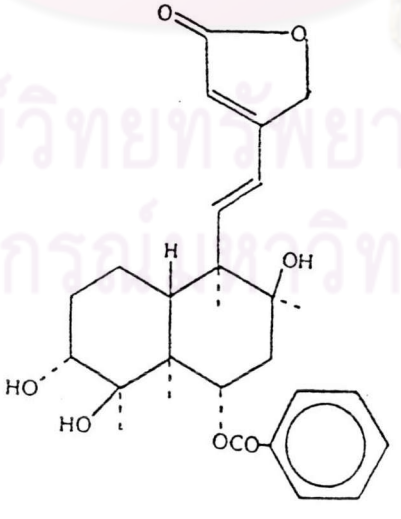

Scuterivulactone D (Kizu et al, 1987)
(Scutellaria rivularis)

4. Neoclerodane type diterpenoid lactone

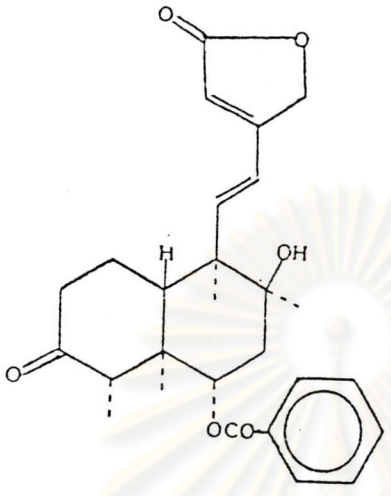

Scutellones E (Lin et al, 1988)

(Scutellaria rivularis)

5. Diterpenoid furanolactone

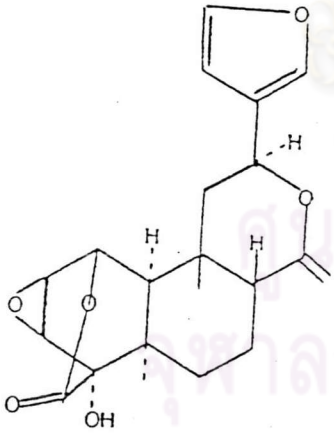

Jateorin (Bhatt et al, 1990)

(Tinospora cordifolia)

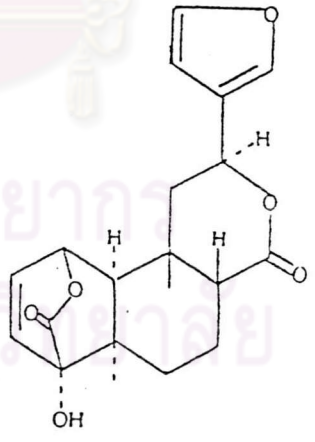

Columbin (Hanuman, Bhatt and Sabuta, 1986)

(Tinospora cordifolia)

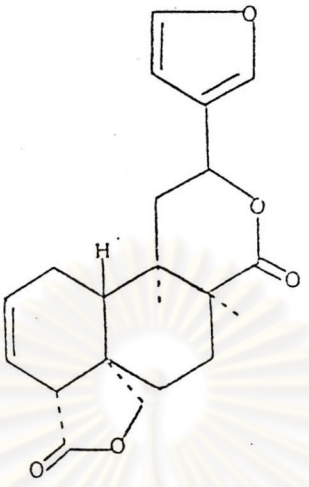

Salverin (Hanuman, Bhatt and Sabata 1986)

(Tinospora cordifolia)

6. Norditerpene lactone

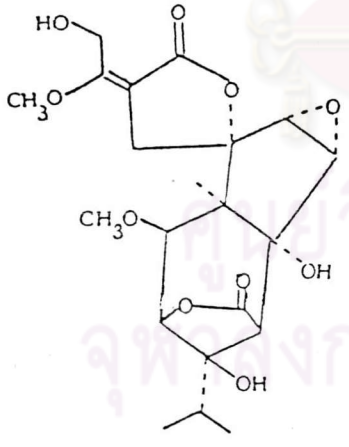

Picrodendrin A (Ohmoto et al 1989)

(Picrodendron bactatum)

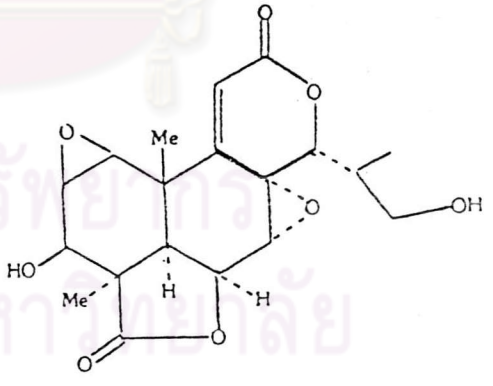

Salignone (Matlin, Bittner and Silva, 1984)

(Podocarpus saligna)

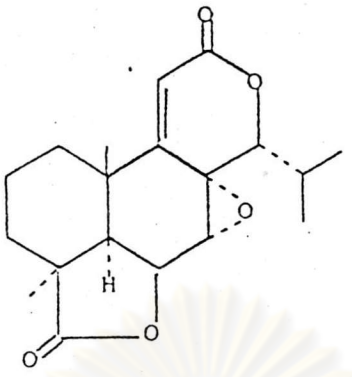

2,3 dihydropodolide (Dasgupta, Burke and Stuart, 1981)

(Podocarpus urbanii)

7. Kaurane type diterpenoid

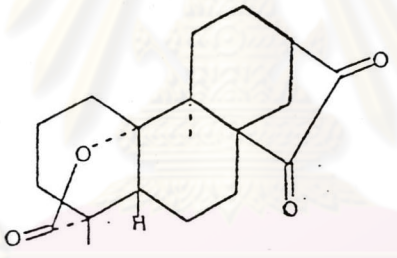

15-oxo-zoaplatin (Delgado, Alvuree and Vivar, 1984)

(Viguiera maculata)

8. Miscellaneous

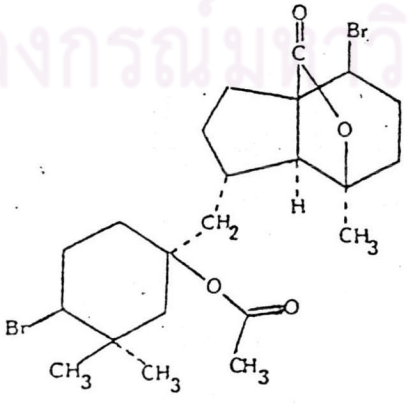

Angasiol acetate (Rahman et al, 1991)

(Aplysia juliana)

## Biosynthesis of diterpenoid lactone

Natural terpenic compounds could be assumed to arise by accepted reaction mechanisms from simple acyclic precursors, squalene, geranyl geraniol, farnesol and geraniol. Fig 2

Geranyl geraniol (GGff) generated from molecules of mevalonic acid (MVA) was specified as the precursors of diterpenes. Akhila et al. (1991) studied biosynthetic pathway of clerodane furano diterpene lactone from 4-R- $H^{3}_{1}$, 2 $C^{14}$ MVA and proposed biosynthetic pathway (scheme 1) and mechanism of cyclisation (scheme 2.)

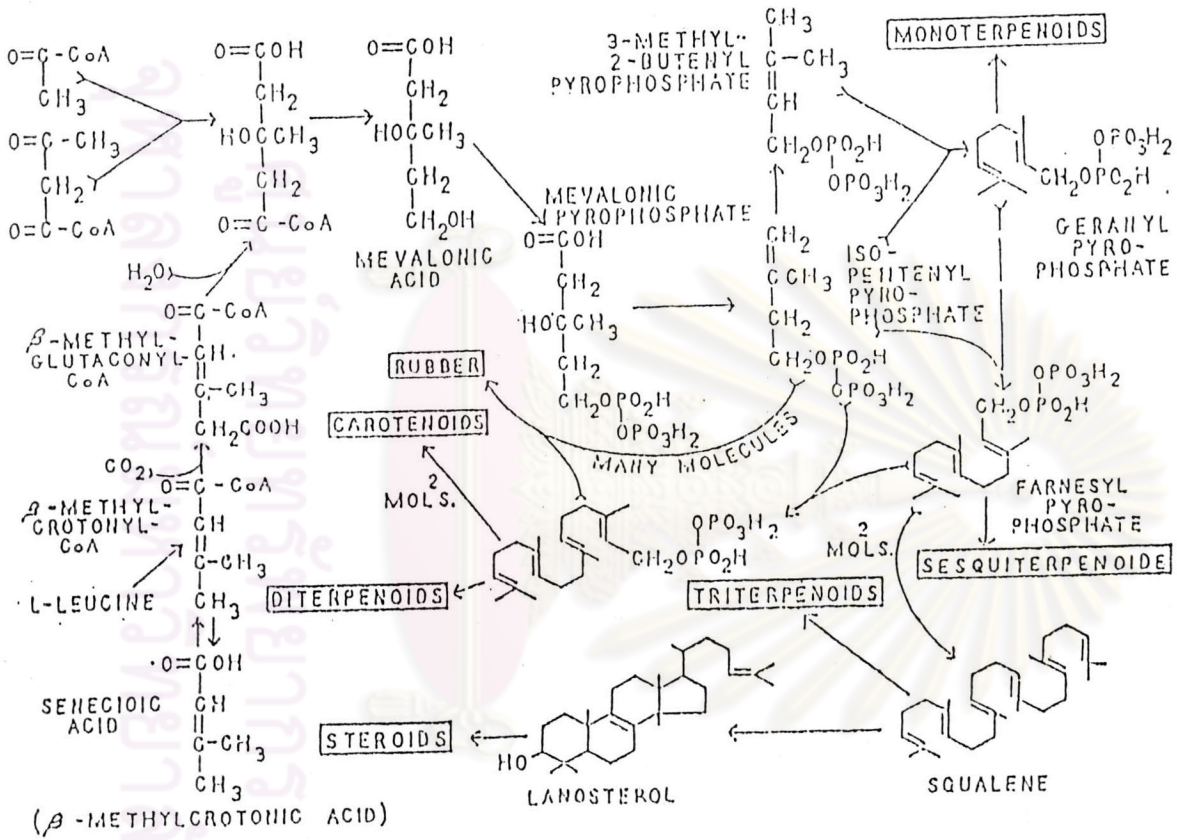


Figure 2 Terpenoid and steroid pathway

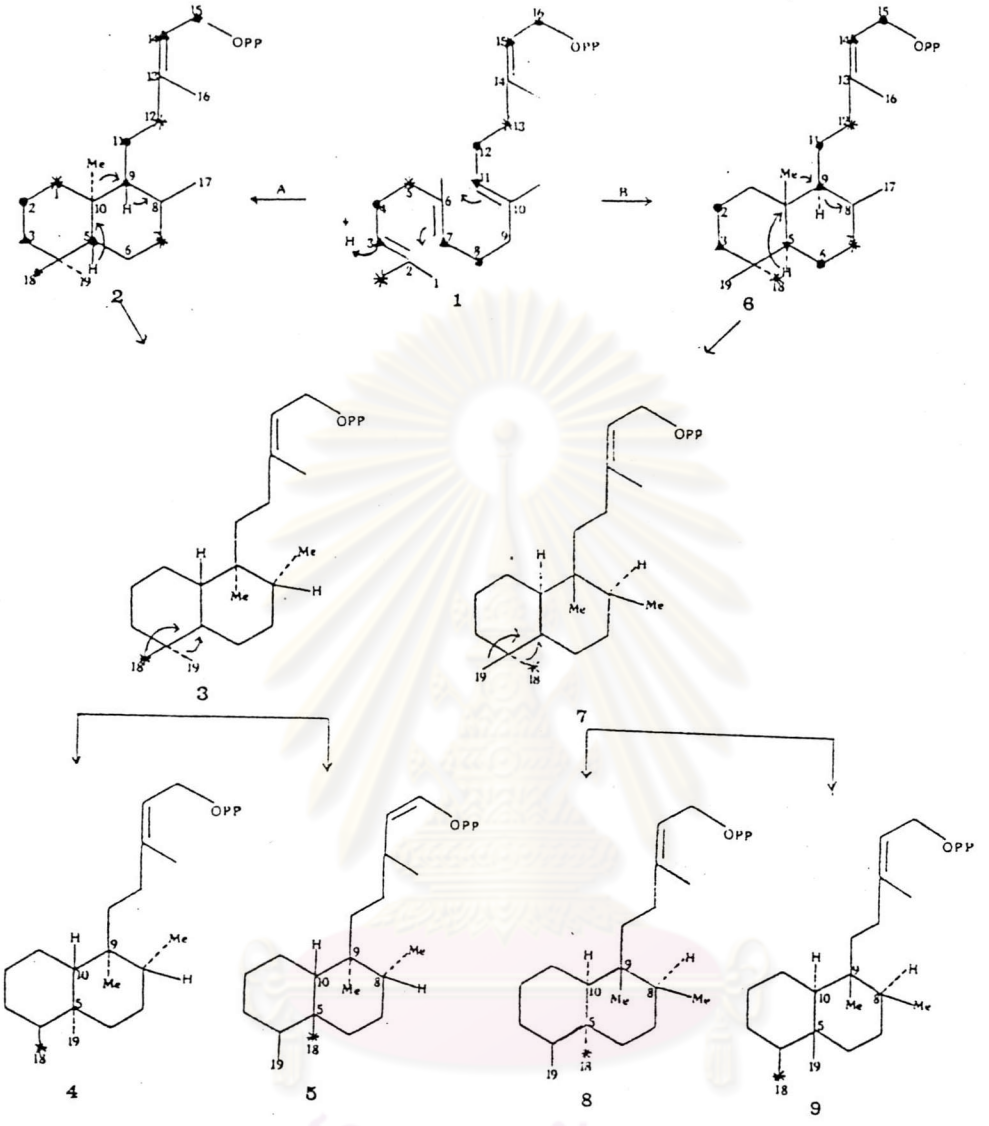

Scheme 1 Suggested biosynthetic pathway to clerodane - furano diterpene lactone skeleton from GGPP. * denotes $^{14}C$ from [2-$^{14}C$] MVA ; ▲ denotes $^{3}H$ from [4R-$^{3}H$] MVA ; ● denotes tracer from MVA having tracer at C-5 . The numbering pattern in GGPP has been changed in diterpene skeletons 9 and 13 in keeping with the traditional numbering system of diterpenes. Compound 9 , 10, 13 and 14 are likely to be enzyme bound species because positive charge units donot exist as such in nature

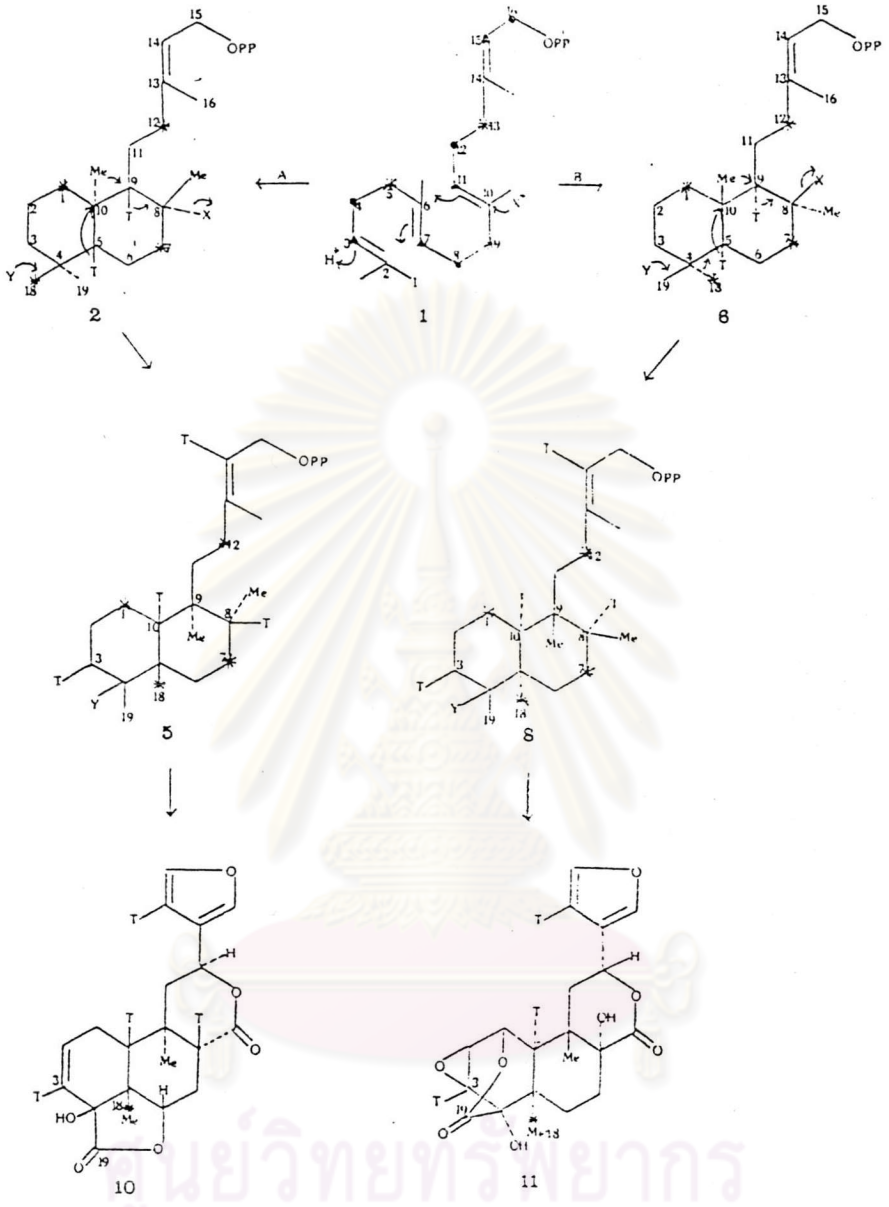

Scheme 2 Suggested mechanism for the cyclisation of GGPP to cis-clerodane compounds.* denotes $^{14}C$ from [2-$^{14}C$] MVA and T denotes $^{3}H$ from [4R-$^{3}H$]

It was well established that C-2 of MVA give rise to C-1, C-7, C-12 and C-18 of the diterpenes, C-4 of MVA to C-3, C-5, C-9 and C-14 and C-5 of MVA to C-2, C-6, C-11 and C-15.

Cis-Clerodane might be formed from GGPP(1) by two route 1 - 2 - 3 - 5 and 1 - 6 - 7 - 8. Similarly, trans-clerodane may be formed from GGPP via 2 - 3 - 4 and 6 - 7 - 9 .

The cyclisation of GGPP started with attack of a nucleophile ($X^-$) or enzyme on C-10 of GGPP from the re-face followed by attack of $\Delta^{10,11}$ on C-6, attack of $\Delta^{6,7}$ on C-2 and finally $\Delta^{2,3}$ accepting an electrophile ($H^+$). This would generate a B-methyl at C-8, a B-H at C-9, and methyl at C-10 and B-H at C-5 of the intermediate 2.

In contrast, a si-face attack of nucleophile ($X^-$)/enzyme on C-10 of GGPP (1) would reverse the stereo chemistry at all the carbon atoms (i.e. C-8, C-9, C-10, C-5, C-4) to produce intermediate 6. Later on 2 and 6 will produce 10 and 11 respectively.

Experimental techniques for $^{13}C$ NMR

Since the early 1980s, modern NMR spectroscopy has become an extraordinarily useful tool for the structural elucidation of unknown organic compound. Some usual experiments are as follow.

1. One-dimensional Nuclear Magnetic Resonance (1-D NMR)

1.1 Proton noise decoupling or broad band decoupling

A proton noise decoupling spectra were obtained by irradiation frequency to remove all carbon-proton scalar coupling. Thus, a significant improvement of the signal/noise ratio is achieved because the signal of insensitive $^{13}C$ nuclei appear at narrow singlet, without any splitting due to $^{1}H$, $^{13}C$ coupling. In addition, the nuclear overhouser effect (NOE) may enhance the signal intensities there by as much as threefold. However, this is accompanied by a complete loss of $^{1}H$ - $^{13}C$ coupling information so that the number of hydrogen atoms adjacent to a carbon no longer been determined.

## 1.2 Gate decoupling technique

A gate decoupling spectra is obtained by turn on the proton decoupler during a pulse delay but turn off during data acquisition. The carbon signals are split owing to the large one bond $^{1}H$-$^{13}C$ coupling constant $^{1}J_{CH}$ (between 120 and 200 Hz), and doublets are observed for CH, triplets for $CH_2$ and quartets for $CH_3$ fragments. These multiplets often contain further fine splitting from couplings over more than one bond and may overlap severely so that an unambiguous assignment is impossible.

## 1.3 Off resonance decoupling

An off-resonance spectra is obtained by irradiation of a selective proton frequency near to the $^{1}H$-resonance range (off-resonance) that partial $^{1}H$ decoupling is achieved. All signals splitting due to carbon-proton couplings are reduced to such an extent that only the large one-bond couplings give rise to a relative small amount of residual splitting.

The disadvantage of this technique becomes apparent when many $^{13}C$ signals exist in a narrow chemical shift range. A situation often occuring in the

spectra of steroid, triterpenoid and other molecules containing many carbon atoms. In spite of the relatively small amount of residual splitting, there is still considerable signal overlap, which many easily obscure any identification of multiplet.

## 1.4 J-modulation or Attach Proton Test (APT)

The experiment evolves proton coupled during the first delay and proton decoupled during the second delay and acquisition periods. During the first proton coupled delay, the two vectors for a particular carbon will process in the rotating frame at a frequency of J/2 ahead of, or behind, the chemical shift frequency. The angle through which the vectors rotate will therefore be control by both the CH coupling constant, J, and the delay time. Heteronuclear decoupling during the second delay period which follow the pulse will switch off the J-coupling and remove the distinction between the two vector, that collapse to a single vector. The amplitude of the resulting singlet will depend only upon the angle $\theta$, magnetization to rotate. In fig. 5 the amplitudes of a doublet, a triplet and a quartet are showed as a function of the delay, tD. At the time $tD = J^{-1}$ the magnetization

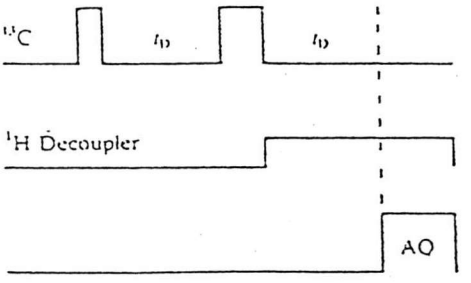


Figure 3 The J- modulated spin-echo sequence

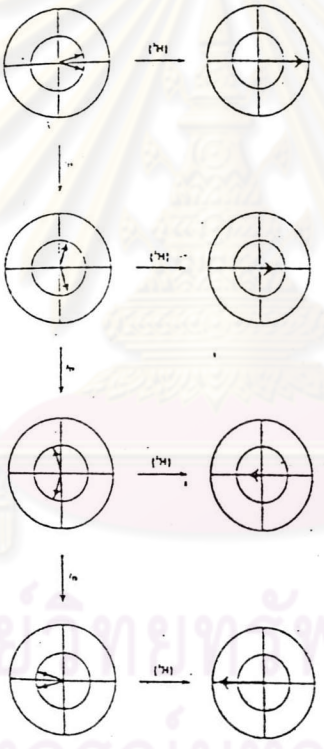

Figure 4 The effect of J modulation on the amplitude of a signal after decouping $\{^1H\}$. In the top case, only a short delay is included and the vector sum is close to the normal value. As the delay is increased, the sum decreases, goes through a null, and inverts.

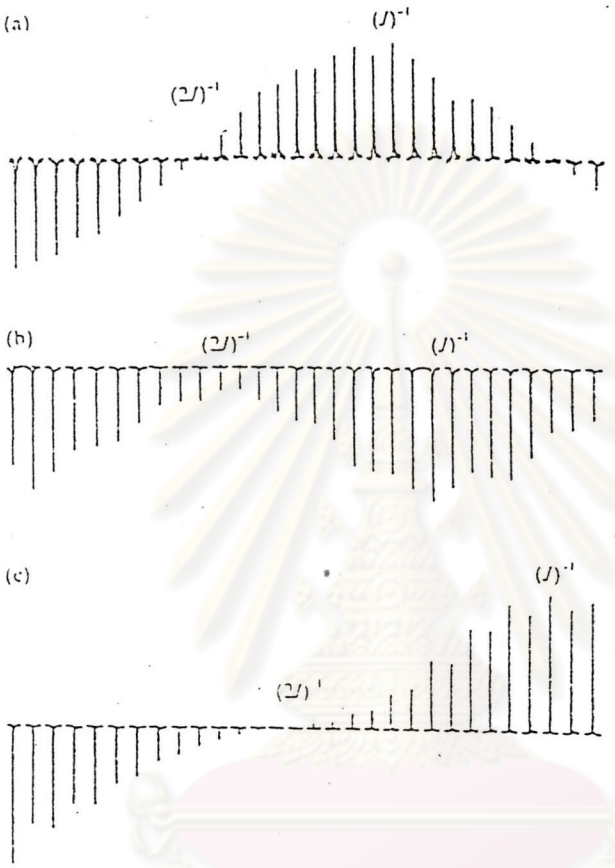


Figure 5 The effect of the J- modulated spin-echo sequence on $^{1}H$ coupling $^{13}C$ multiplets . tD is increased by 0.25 ms in successive traces. (a) the doublet of $CHCl_3$ J =213 Hz;(b) the triplet of $CH_2Cl_2$ J= 179 Hz; (c) the quartet of $CH_3OH$, J=138 Hz

components are realigned for all three coupling situation the phase of the methine and methyl signals is opposite to that of the methylene signal.

A spectrum where the amplitude of the carbon signal depends on the delay, the time dependent amplitude, or amplitude modulation, is a function only of $J_{CH}$, and the number of attached protons. Chemical shift evolution is switched off by using the spin-echo. The experiment is referred to as a J modulated spin echo or the attached proton test (ATP)

## 1.5 Insensitive Nuclei Enhanced by Polarization Transfer (INEPT)

Population transfer or polarization transfer has the basic principle that pertubation of the population distribution of spin A will have an effect on the population of spin which are J coupled to A. The pertubation is created by allowing the evolution of magnetization vectors between pulses.

INEPT is a sequence which allow simultaneous polarization transfer from all proton to all nuclei with the same coupling and number of attached proton. The basic pulse sequence may be written.

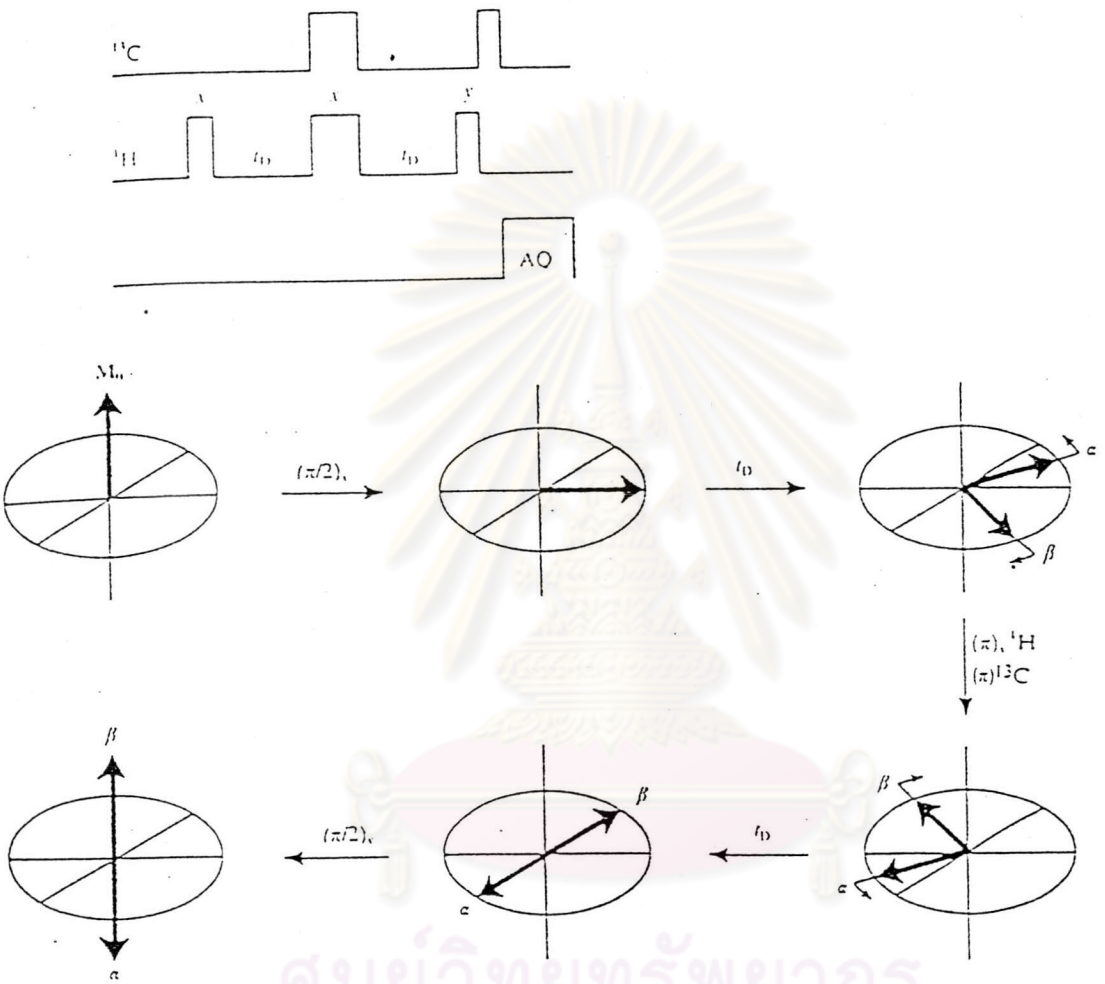


Figure 6 Vector diagram for the protons during the INEPT sequence.

$^{1}H$ $(\pi/2)x$ - tD-$(\pi)x$ - tD - $(\pi/2)y$

$^{13}C$ $\pi$ - tD - $(\pi/2)$ - Acquire

The result of a single INEPT sequence, then is non-selective polarization transfer from proton to all carbons with the appropriate $^{1}H$- $^{13}C$ coupling. All $^{1}H$ chemical shift effects are removed from the carbon spectrum and each carbon doublet will have the 5:-3 intensity pattern. The INEPT sequence is usually applied in a slightly different form, the phase of the second $\pi/2$ pulse being alternated between +y and -y. The phase alternation producing an intensity pattern of 8:-8 or 1:-1 for the observed doublets. Triplets and quartets due to $CH_2$ and $CH_3$ groups are similarly modified in appearance,becoming 1:0:-1 and 1:1:-1:-1 respectively.

## 1.6 Distortionless Enhancement by Polarization transfer

As a polarization transfer technique DEPT is useful for the observation of low $\gamma$ nuclei which are J couple to $^{1}H$, $^{19}F$ or $^{31}P$. It can also produce separate carbon subspectra for methyl methylene and methine signal. The pulse sequence is

$^{1}H$ $(\pi/2)x$ - tD - $(\pi)x$ - tD - $(\theta)y$

$^{13}C$ $(\pi/2)x$ - tD - $(\pi)x$ - tD - Acquire

The delay, tD, is set to $(2\ J_{CH})^{-1}$, and the whole sequence requires phase cycling to ensure maximum cancellation of natural magnetization and pulse errors. Acquisition may be performed with or without broadband proton decoupling.

The intensities of methine, methylene, and methyl signals, depend differently on the width of the $\theta$ pulse, it is this factor that forms the basis of spectrum editing with DEPT. Fig. 7 shows the variation of intensity with $\theta$, using representative methine, methylene and methyl signals of cholesterol as an example. Methyl and methylene groups each have maximum intensity when $\theta = \pi/4$ and are nulled for $\theta = \pi/2$ while the intensity of a methine group reaches a maximum when $\theta = \pi/2$. Methylene groups reach a negative maximum when $\theta = 3\pi/4$. If DEPT is to be used to acquire a routine $^{13}C$ spectrum, then $\theta$ should be set to $\pi/4$, a value that will give useful enhancements for all protonated carbons.

DEPT has several practical differences from the INEPT sequences.

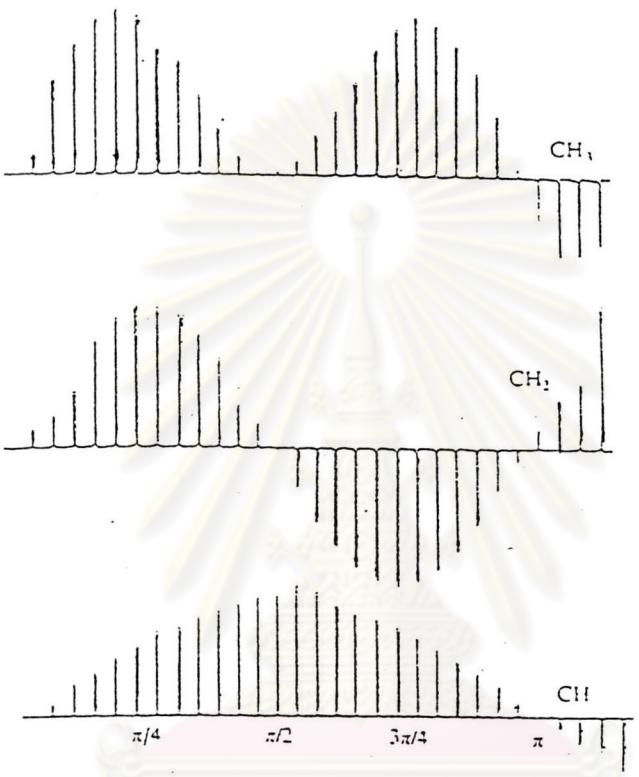


Figure 7 Plots of signal intensity versus θ for a methine, methylene and methyl carbon of cholesterol

a) INEPT given 1:0:-1 and 1:1:-1:-1 multiplets for $CH_2$ and $CH_3$ groups respectively, whereas DEPT gives the more familiar 1:2:1 triplets and 1:3:3:1 quartets; this is the origin of 'distortionless' in the name. In practice, one rarely acquires proton coupled spectra, so this advantage is of little practical consequence.

b) DEPT is less sensitive to a precise matching of the delays and coupling constants, INEPT depends for its editing powers on setting tD to a value which is critically dependent on $J_{CH}$, while DEPT is relatively insensitive to mis-setting of the delays.

## 2. Two-dimensional nuclear magnetic resonance (2D NMR)

2D NMR spectra are obtained by 4 steps; preparation period, evolution period, mixing period and detection period.

The nucleus in preparation period are spinning in equilibrium state while a pulse is given to the system in the variable time to exited the nucleus. The relaxation of the excited state nucleus will evolve free induction decay (FIDs). A pulse is given again to the system to get the second FID. The second FID is in time domain function

S(t1, t2) and changed to frequency domain function S(f1, f2) by fourier transformation.

The fourier transformation is repeated to array the frequency domain again from

$$s(t1, f2) \rightarrow s(f2, t1)$$

$$s(f2, t1) \rightarrow s(f2, f1)$$

and achieved 2-D spectra

There are two options available for presenting 2D spectra, one is stacked plot (Fig. 8). The second and generally more preferred option, is the contour plot. (Fig. 9)

### 2.1 $^{1}H$, $^{1}H$ correlated (H,H COSY) 2D NMR spectra

COSY (correlated spectroscopy) experiment is the process of coherence transfer in which magnetization is transfer between couple spins. In the homonuclear experiment where H, H spin-spin couplings provide the means for the transfer of magnetization and the nucleus spins are alway coupled, therefore coupling information may always be transferred from one spin to another.

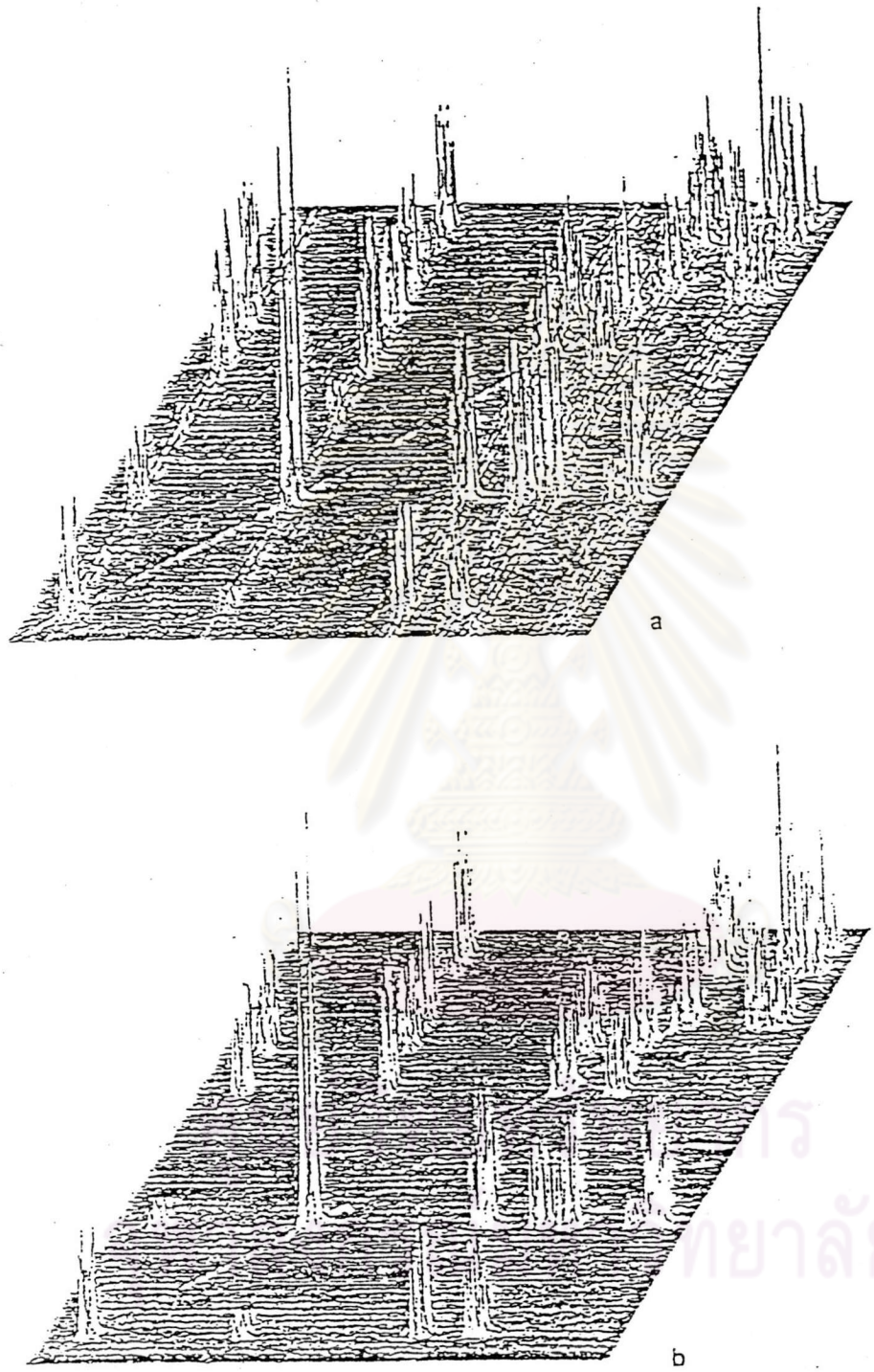


Figure 8 Stacked plot of an H,H COSY spectrum of N-methyl-benzoisocarbostyril , aromatic region only (a) not symmetrized (b) symmetrized

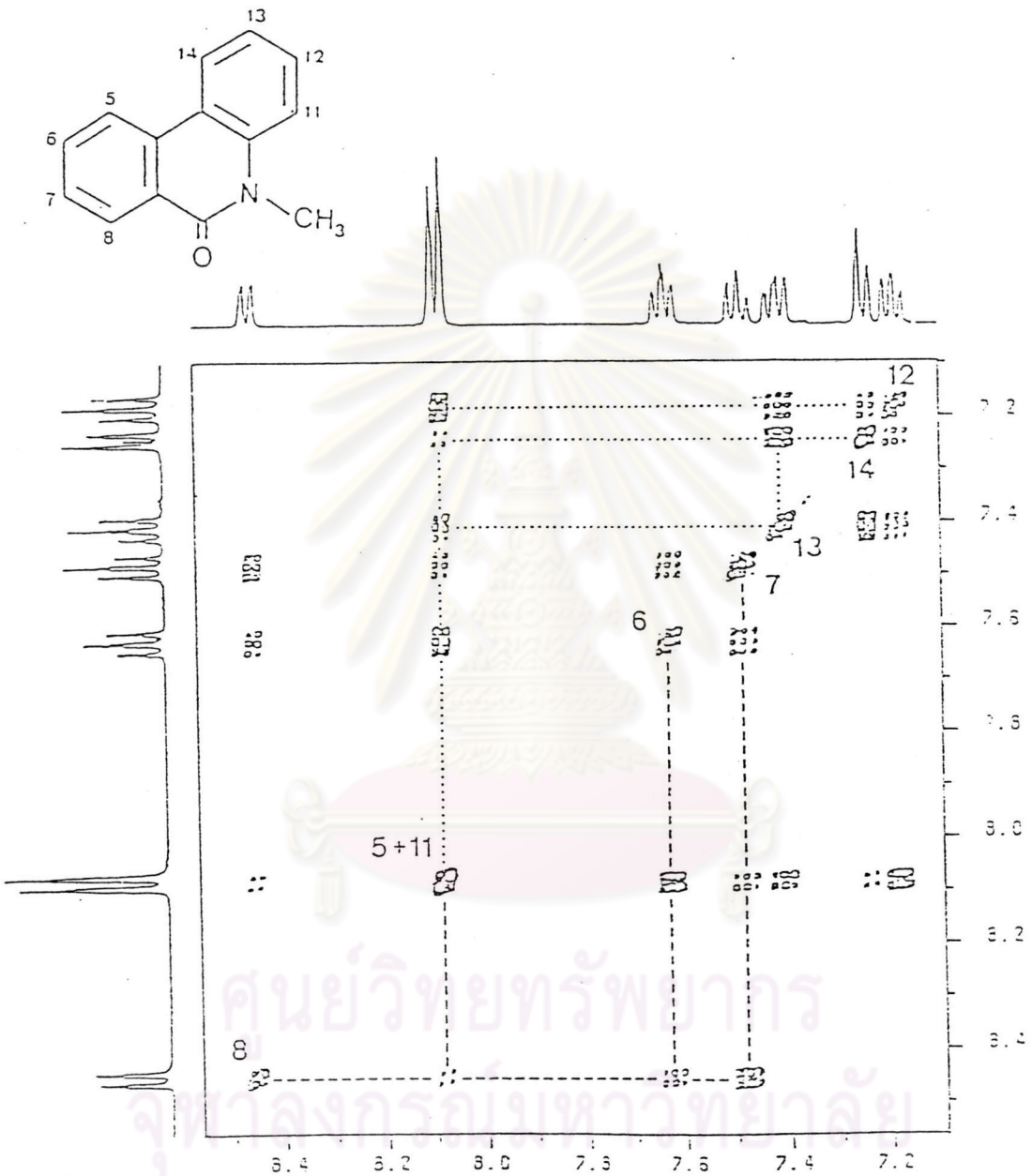


Figure 9 Contour plot of an H,H COSY spectrum of N methyl-benzocarbostyril, aromatic region only , symmetrized

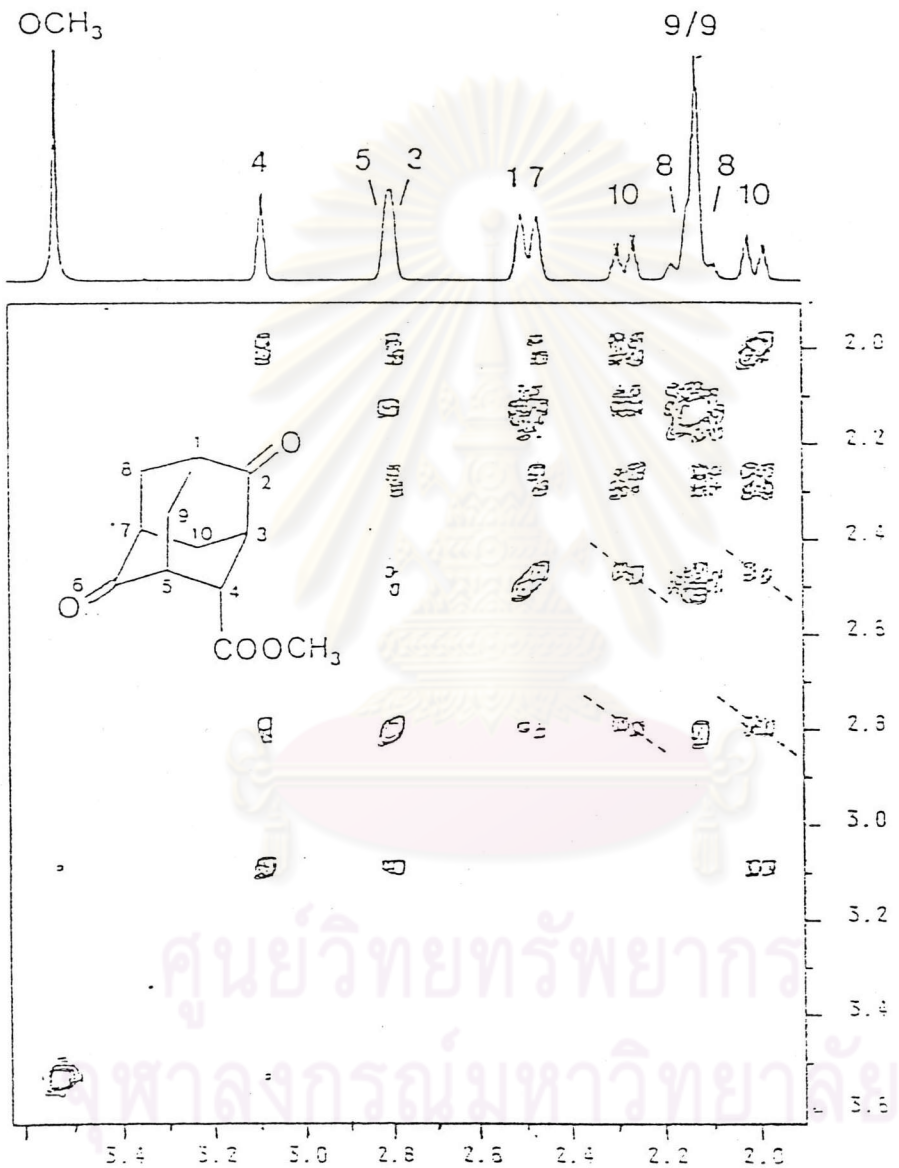


Figure 10 H,H COSY spectrum (COSY 45) of 4 methoxycarbonyl-adamantane-2,6-dione.

Two basically different types of signals appear in $^{1}H$, $^{1}H$ COSY spectra. The diagonal peak represent the original spectrum as obtained in a 1D experiment. which prove the existence of scalar (through-bond) couplings between nuclei. The corresponding coupling partners can be found by drawing horizontal and vertical line starting at the cross peak until the diagonal is intersected; these positions are the signals of the coupling partners. Owing to the symmetry of the spectrum this procedure can be performed in either the upper left or the lower right triangle (Fig.9)

If the signals of coupling partners are close to each other, that is, if they have very similar chemical shifts the corresponding cross peak is located very near to the diagonal and many be obscured by overlap of the diagonal peaks. In such case there are variants and improvements of the cosy pulse sequence to alleviate the situation. In the so-called cosy $45^{o}$ varient the second pulse is not a $90^{o}$ but a $45^{o}$ pulse, decreasing the extension of the diagonal peaks. (Fig.10)

## 2.2 $^{1}H$, $^{13}C$ Correlated (H, C COSY) 2D NMR spectra

The H, C COSY measurement is extremely important, since it connects $^{1}H$ signals in the F1 dimension with $^{13}C$ signal in F2. The pulse sequence is shown in

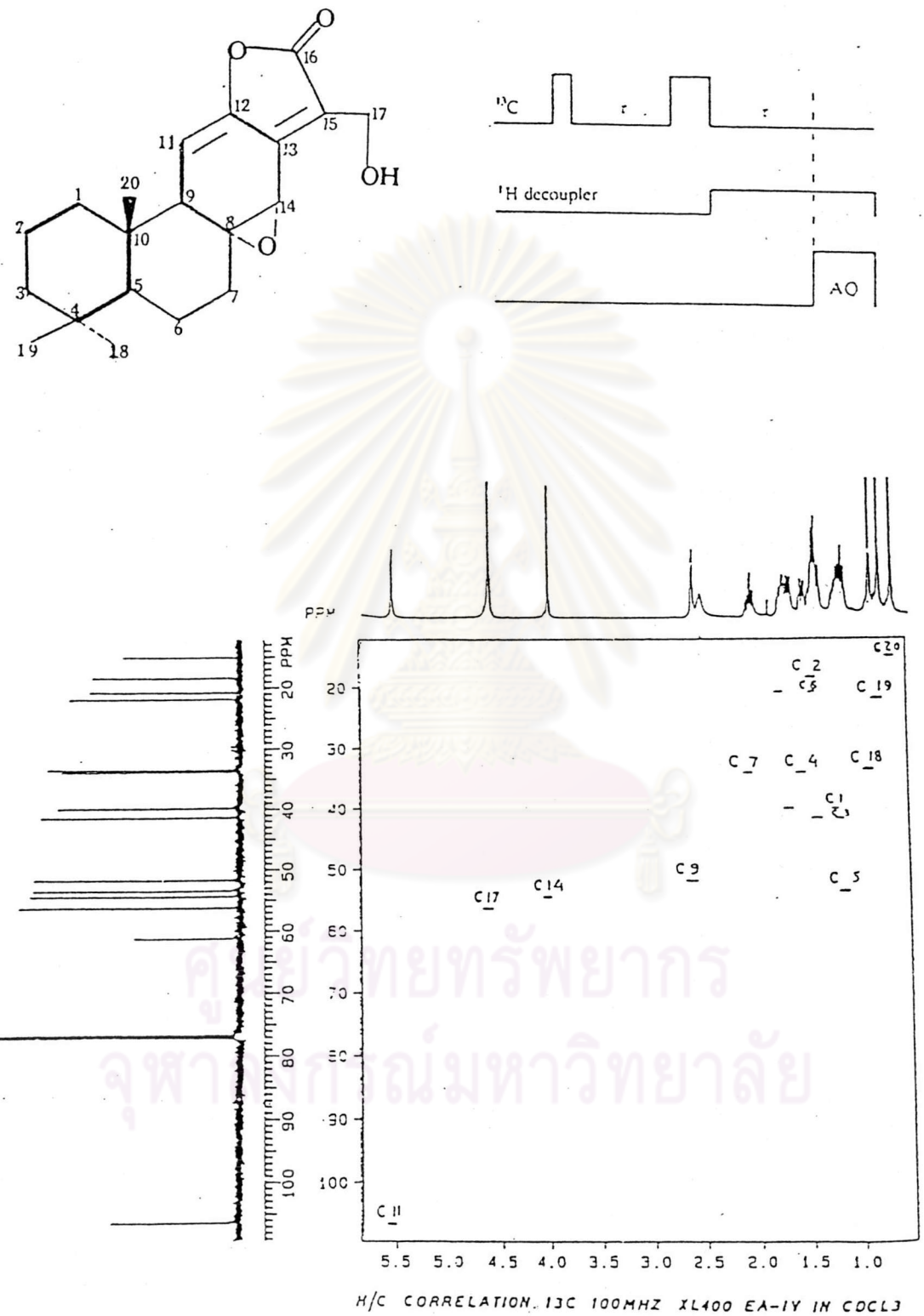


Figure 11 Pulse sequence of C,H correlation experiment and C,H correlation spectrum of caudicifolin

Fig.11 The $180^{o}$ carbon pulse has the effect of decoupling in the F1 dimension, whereas proton noise decoupling provides decoupling in the F2 dimension.

H, C Correlated spectra of caudicifolin are shown in fig.11

## 2.3 COLOC spectra

H, C COSY is largely limited to one-bond couplings and becomes insensitive if it is optimized to a small long-range $^{1}H$, $^{13}C$ coupling constant. In such case the corresponding delay times have to be quite long, so, owing to transversal relaxation, the magnetization is more or less delayed at the end of the pulse sequence before it can be monitored, that can be achieved by COLOC (Correlation Spectroscopy via Long-Rang Couplings). This technique is particulary suitable if the molecule contains quaternary carbons , since $^{1}H$, $^{1}H$ couplings influence signal intensities of COLOC peaks in a way not easy to predict, COLOC should preferably be applied to molecules or molecular fragments bearing only few hydrogen atom.

In fig.12 COLOC of Picrodendrin A shows the two and three bond correlations.

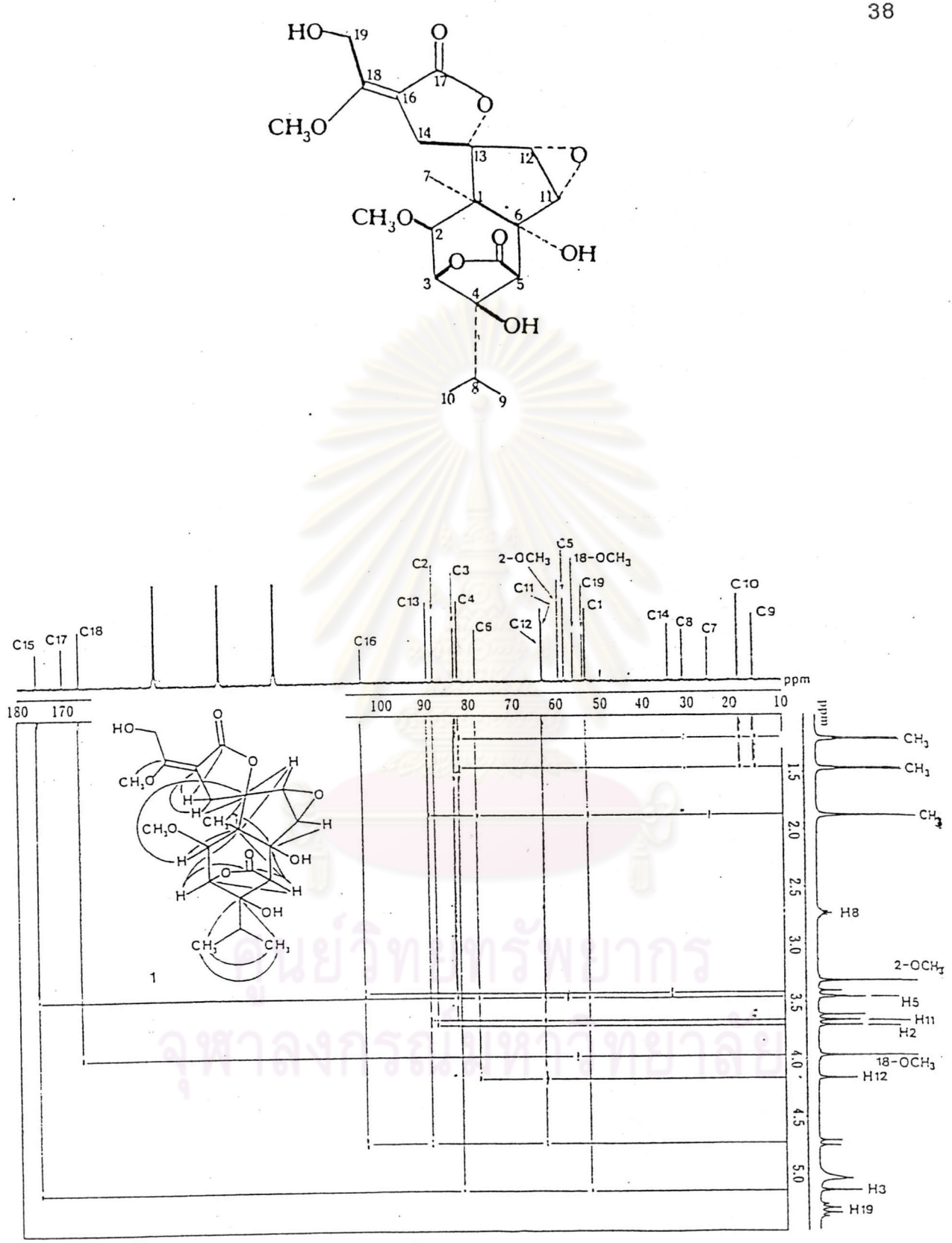


Figure 12 $^{1}H$-$^{13}C$ Long-Range 2D COSY Spectrum and Two and Three -Bond Correlations of Picrodendrin A

## 2.4 2D $^{13}C$, $^{13}C$ (C, C COSY) INADEQUATE spectra

Structural elucidation of an unknown organic compound or a natural product implies establishing the connectivity of the atoms in the carbon skeleton. The method previously only achieve this goal indirectly. For example, first by evaluation of the H, H COSY spectrum, the connectivity of the proton is established, then in a second step, H, C COSY and COLOC experiments show to which carbon these proton are bonded so that the C, C connectivity is finally obtained.

The problem for obtaining the C, C connectivity spectra directly from $^{13}C$, $^{13}C$ coupling are the rarity of $^{13}C$ isotope (only one in about 8000 molecules) contains two $^{13}C$ nuclei in two ascertained positions) and the signals from $^{13}C$ satellites in the $^{13}C$ NMR spectrum can easily be overlapped by the main signal arising from molecules containing only a single $^{13}C$ nuleus. In addition rotation side bands and peaks from traces of impurities may obscure the identification of the $^{13}C$ satellites.

INADEQUATE (Incresible Natural Abundance Double Quantum Transfer Experiment) technique has double quantum filter which suppresses strong singlet of if isolated $^{13}C$ nuclei from $^{13}C$ NMR spectra and then increase the intensity of settelite line of $^{13}C$-$^{13}C$ coupling.

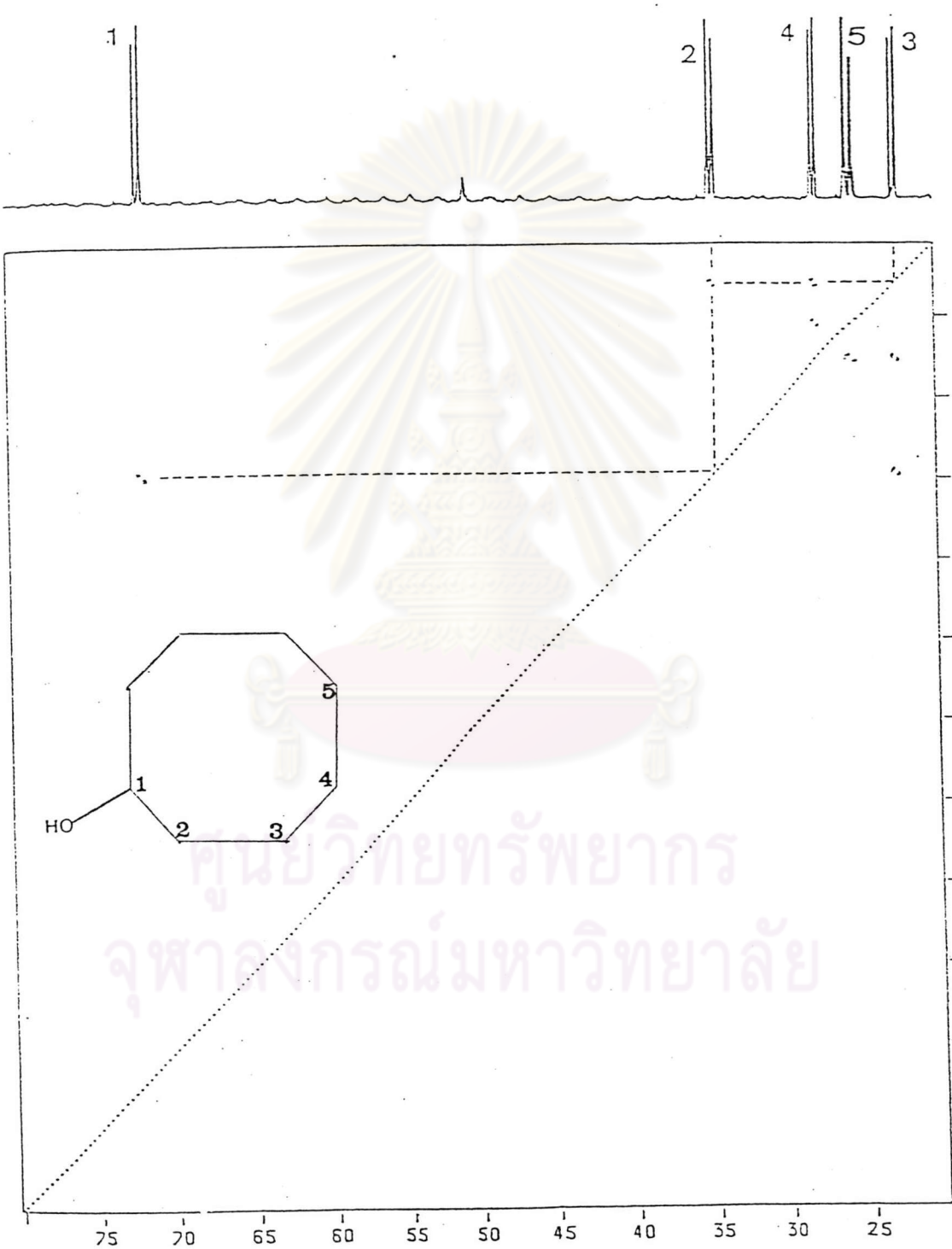


Figure 13 2D INADEQUATE spectrum of cyclooctanol; the 1D spectrum on the top of the plot is the projection ,not the normal $^{1}H$ broad-band decoupled $^{13}C$ NMR spectrum.

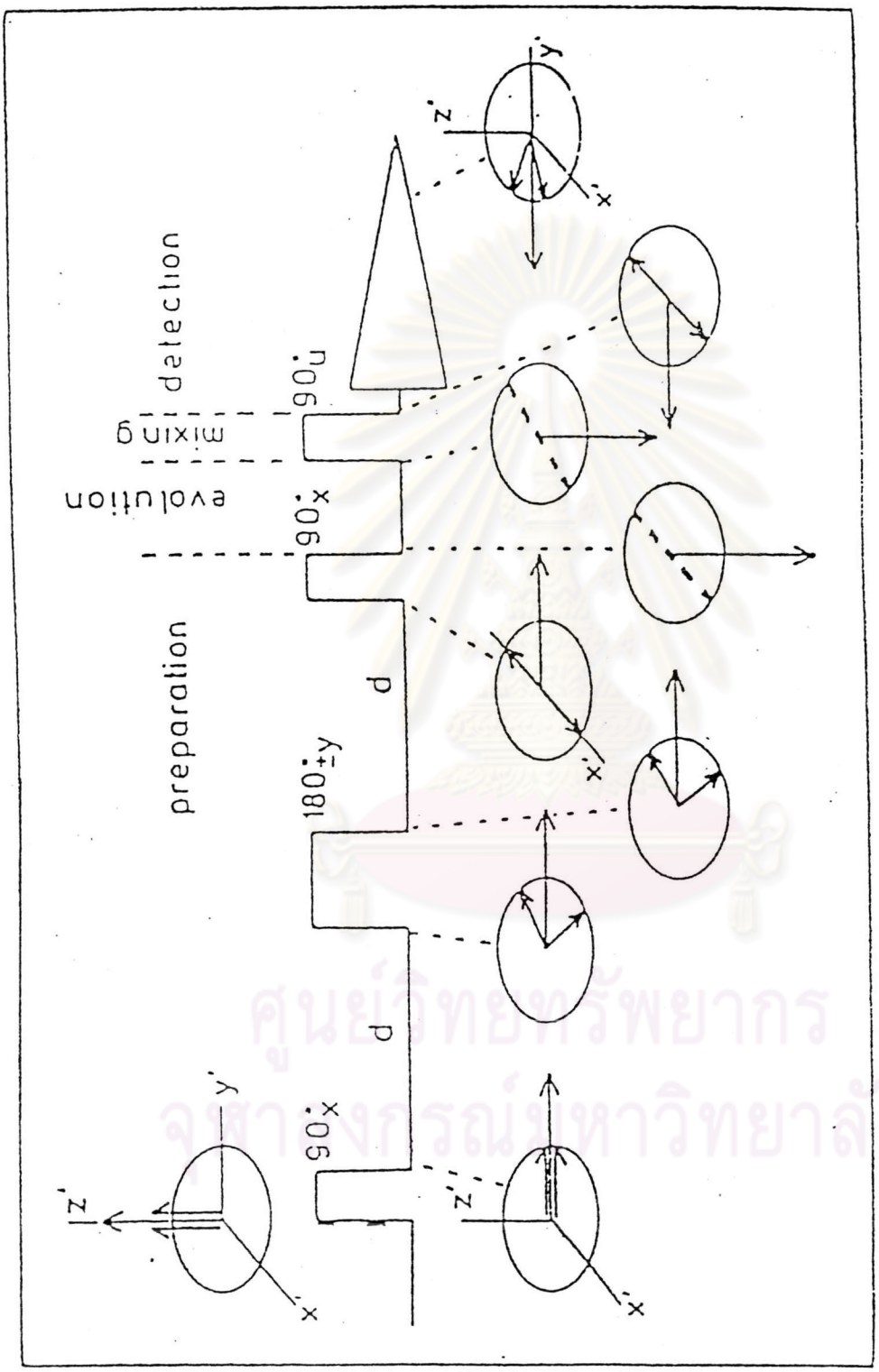


Figure 14 Pulse sequence of the 2D INADEQUATE

This technique also removes rotation side bands and signals from impurities.

The 2-D INADEQUATE has the pulse sequence as following.

$$90^{\circ}x\text{-}d\text{-}180^{\circ}x\text{-}d\text{-}90x\text{-}t1\text{-}\alpha x\text{-detection}$$

The 2-D INADEQUATE spectrum of cyclooctanol is in fig.13 In an evaluation similar to that of the H, H COSY spectra, the connectivity of all carbons in cyclooctanol can be obtained starting with the obvious signal to assign, namely C-1. Below the corresponding doublet in the trace above the 2D plot, there is a cross peak leading to C-2 following the horizontal dashed line until it intersects the diagonal (dotted line). From here a vertical dashed line identifies the C-2 signal. For C-2 there is another cross peak from which a new horizontal dashed line is drown making another intersection with the diagonal that end up at C-3. The signals of C-4 and C-5 can be identified analogously.

2-D INADEQUATE experiment is very time consuming often it requires one or two days of spectrometer time. Consequently such measurement are performed only when indirect methods for establishing C, C connectivities fail.

## 3 NOE Difference Spectra

Since the early 1980s, the so-called NOE difference technique has been used to substract free induction decays (FIDs) obtained with pulse fourier transform (PFT) spectrometers, both with or without double resonance irradiation. These difference spectra contain signals only of such nuclei which suffer from NOE-induced intensity changes, all other are cancelled thus, even very small intensity differences can be reliably monitored, and there is no overlapping of uninvolved signals.

The foregoing is demonstrated in fig.16 The acetate of a benzodiazepinone derivative has been nitrated. The question is whether the newly introduced nitro group is situated at position 7 or 8. This problem cannot be solved by establishing the H, H connectivity, since there are no detectable couplings between the aromatic and aliphatic protons.

Irradiation of the acetoxy methyl protons affords significant intensity enhancements for H-4 and for one of the aromatic protons, which apparently does not posses an ortho-positioned $^{1}H$ neighbor since the signal is a narrow singlet. Owing to spatial proximity, this can only be H-6, so, it has to be concluded that the nitro group is attached to C-7. This simple experiments, requiring only a few minutes of spectrometer time.

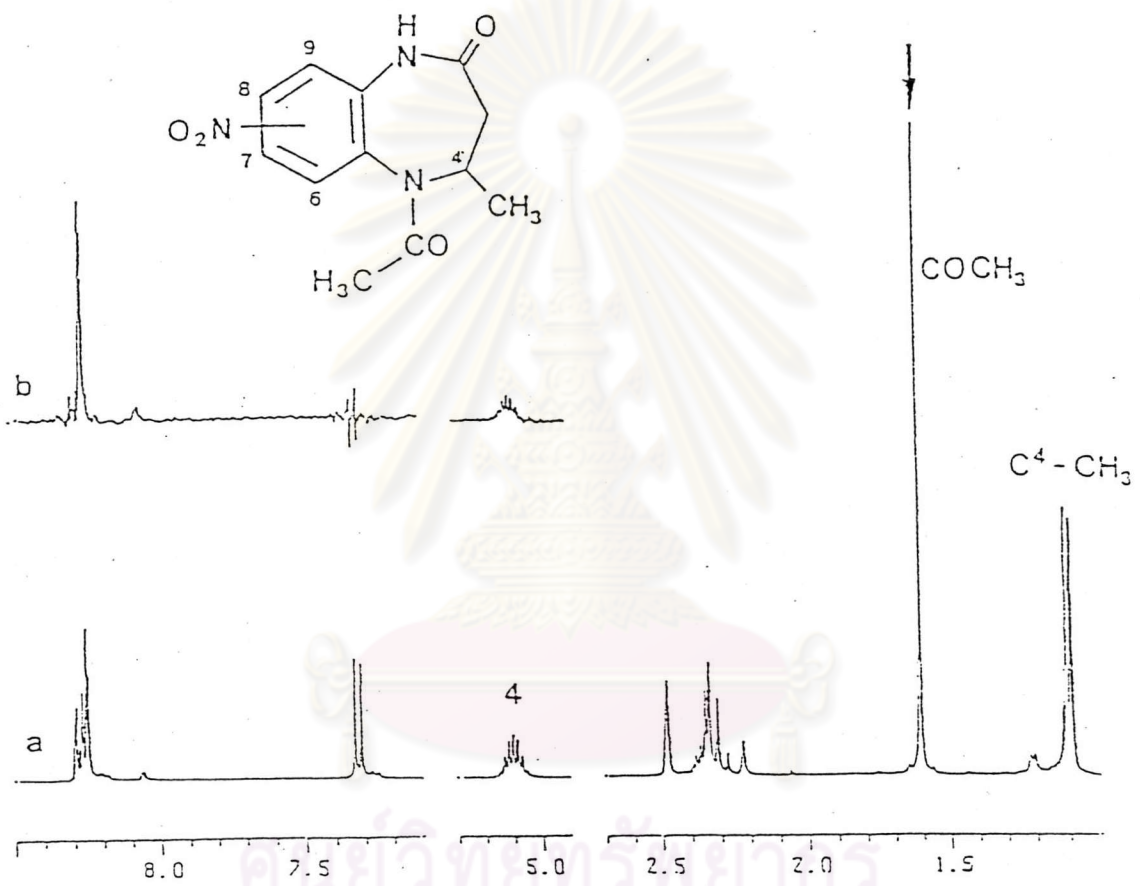


Figure 15 a and b. NOE difference experiment with a nitrated benzodiazepinone derivative ,in DMSO-d6 ;a $^1H$ NMR spectrum ;b NOE difference spectrum with irradiation at the position of the acetoxy methyl signal(mark by the arrow)

This techniques can also be derived from 2-D (the so-called NOESY) experiments. These spectra are very similar to H, H COSY spectra, the cross peaks, however, do not indicate scalar (through bond) but rather, dipolar (through space) coupling.

Fig.16 show the spatial proximity between the proton of the C-1 and C-11 position, as well as the methoxy group and aromatic proton at the C-8 position and between the C-7 methylene. This observation revealed that the methoxy group is attached to C-9 in aromatic ring.

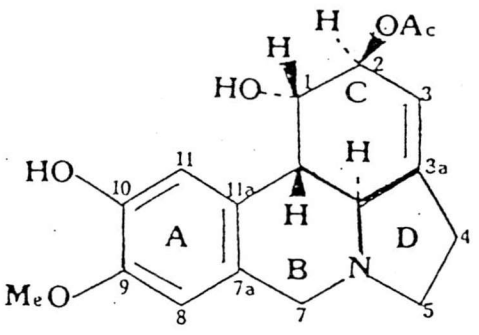


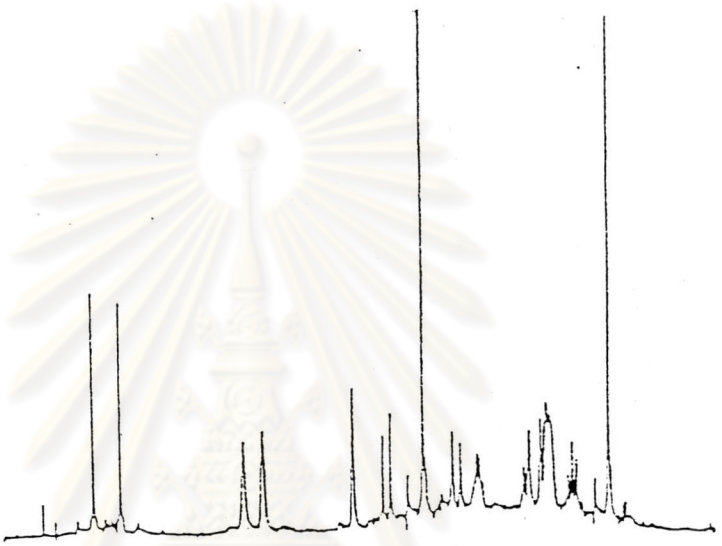

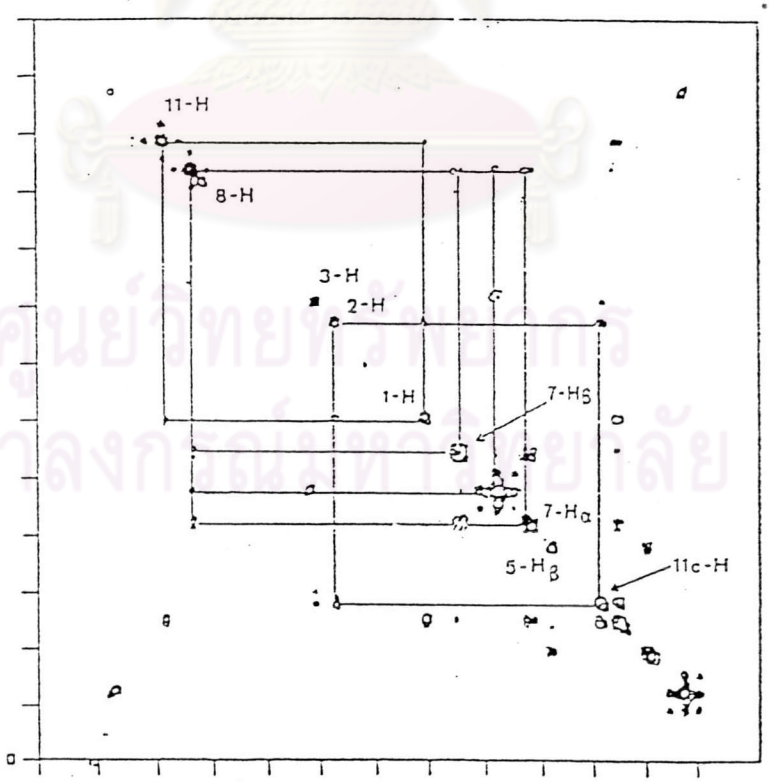


Figure 16 NOE 2D spectrum of 2-o-acetylpseudolycorine